Photodynamics of the Paterno–Büchi cycloaddition of stilbene to quinone. Unusual modulation of electron-transfer kinetics by solvent and added salt

Stephan M. Hubig, Duoli Sun and Jay K. Kochi

Department of Chemistry, University of Houston, Houston, Texas 77204-5641, USA

Received (in Cambridge) 8th December 1998, Accepted 19th January 1999

Oxetanes are produced in the Paterno–Büchi cycloaddition of stilbene (**S**) to quinone (**Q**) *via* an efficient photo-induced electron transfer. Kinetics analysis of the time-resolved absorption spectra over three distinctive (ps, ns, μs) timescales establishes the coupling (k_C) of the initially formed ion-radical pair ^{3}[**S**$^{+\bullet}$, **Q**$^{-\bullet}$] to the 1,4-biradical $^{\bullet}$**SQ**$^{\bullet}$ as the critical step toward oxetane formation. The (rather slow) rate constant of $k_C \leq 10^7$ s^{-1} in acetonitrile must compete with other faster decay pathways of the ion pair involving ionic separation, ion exchange (with added salt) and back electron transfer. As such, solvent polarity and donicity as well as added salts play an unusually prominent role in modulating the ion-pair microdynamics. Donor–acceptor complexation of the photoexcited quinone with the solvent and *cis*→*trans* isomerization of (*Z*)-stilbene must also be considered in the overall photodynamics of electron transfer.

Introduction

Stilbene cycloaddition to photoactivated chloranil affords the stable oxetane adduct **1** in high yield;[1,2] and it is thus the prototypical example of a synthetically useful Paterno–Büchi coupling[3] of a carbonyl and an olefinic substrate [see eqn. (1)].

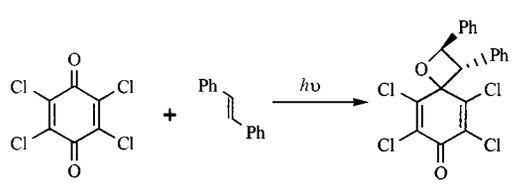

Q **S** **1** (1)

All spectroscopic observations lead to the general conclusion that oxetane formation is not the outcome of a concerted cycloaddition process, but the result of a series of dark reactions following the initial photoactivation of the carbonyl component.[4–13] In the case of the chloranil–stilbene pair,[2] an electron-transfer mechanism is applicable on the basis of the well-known redox behavior of triplet chloranil.[14,15] For example, the photoexcitation of chloranil (**Q**) generates the triplet excited state with unit efficiency[14,16] by ultrafast intersystem crossing ($k_{ISC} \cong 10^{11}$ s^{-1}) from the singlet manifold.[17] The triplet quinone (^{3}**Q***) acts as a powerful oxidant,[18] which readily oxidizes stilbene (**S**)[19] upon diffusional encounter to result in the formation of triplet ion-radical pairs,[14,16,20] as shown in eqn. (2).

$$Q \xrightarrow{h\nu} {}^3Q^* \xrightarrow{S} {}^3[S^{+\bullet}, Q^{-\bullet}] \qquad (2)$$

As such, the photocoupling between chloranil (**Q**) and stilbene (**S**) is particularly suited to study the fate of the triplet ion pair since both the chloranil anion radical (**Q**$^{-\bullet}$)[22] and the stilbene cation radical (**S**$^{+\bullet}$)[23] exhibit well-known (characteristic) absorptions, which can be readily identified and monitored by time-resolved spectroscopy. Since the competition between the various reaction pathways of the triplet ion-radical pair is critical to the overall efficiency of the Paterno–Büchi coupling, the quantum yield of the oxetane formation in eqn. (1) and its remarkable dependence on solvent and salt effects must be related to the dynamics of the ion-pair intermediate in eqn. (2). Accordingly in this study, we show how solvent polarity and donicity control the formation as well as the reaction path of the ion-radical pair to such a degree that the quantum yields of oxetane formation can vary by several orders of magnitude. In fact, even the complete inhibition of the Paterno–Büchi coupling of stilbene and chloranil is shown to occur in certain solvents or by the addition of inert salt. Since (*Z*)- and (*E*)-stilbene both form the same *trans*-oxetane upon cycloaddition to photoactivated chloranil,[1] we also investigate the role of *cis*→*trans* isomerization of the stilbene cation radical as an additional reaction path.

Results

I. Oxetane formation *via* the [2+2] cycloaddition of stilbene to photoactivated chloranil

A. Product analysis and determination of photochemical quantum yields. The photocoupling of chloranil and stilbene was achieved by irradiation of an equimolar (0.1 M) solution of (*E*)-stilbene and the quinone in benzene with a high-pressure mercury lamp at wavelengths $\lambda_{exc} > 370$ nm. Under these conditions, stilbene did not absorb the actinic light, and selective photoactivation of the quinone was ensured. Upon complete consumption of the chloranil (as revealed by periodic HPLC analysis), a single photoproduct was isolated in 86% yield, and it was identified as the *trans*-oxetane (**1**)[1,2] in eqn. (1). The quantum efficiency of the oxetane formation was determined with the 436 nm line of the mercury lamp as irradiation source. A concentrated (0.15 M) ferrioxalate solution[24] was used as the chemical actinometer (see the Experimental section) to determine the quantum yield of $\Phi = 0.10$ for oxetane formation in benzene solution.

B. Solvent and salt effects on the quantum efficiency of oxetane formation. The photocoupling of stilbene with chloranil was carried out in seven solvents of different polarity and donicity, and the effects of added salt (tetra-*n*-butylammonium hexafluorophosphate) were investigated in dioxane and tetrahydrofuran solutions. As shown in Table 1, the quantum yields (Φ) of oxetane formation varied substantially depending on the

Table 1 Solvent and salt effects on the quantum efficiency for oxetane formation by photocoupling of stilbene and chloranil[a]

No.	Solvent	Φ[b] [±0.01]	IP[c]/eV	DN[d]/kcal mol^{-1}	ε[e]	$E_T(30)$[f]/kcal mol^{-1}
1	Acetonitrile	0	12.20	14.1	37.5	46.0
2	Dichloromethane	0.01[g]	11.35		9.08	41.1
3	Tetrahydrofuran	0.05	9.42	20.0	7.58	37.4
4	Dioxane	0.34	9.13	14.8	2.25	36.0
5	Benzene	0.10	9,23	0.1	2.28	34.5
6	Toluene	0.06	8.82		2.44	33.9
7	*p*-Xylene	0.01	8.44		2.27	33.2
8	Dioxane (0.1 M TBA PF_6)	0.05				
9	Tetrahydrofuran (0.1 M TBA PF_6)	0.01				
10	Tetrahydrofuran (1 M TBA PF_6)	0				

[a] Irradiation of an equimolar (0.1 M) solution of chloranil and stilbene at λ_{exc} = 436 nm at room temperature. [b] Quantum yield of oxetane formation determined by ferrioxalate actinometry (see text). [c] Ionization potential from ref. 26. [d] Gutmann's donor number from ref. 25. [e] Relative permittivity from ref. 25. [f] Dimroth–Reichardt parameter from ref. 25. [g] Saturated solution of chloranil (0.017 M).

solvent used. For example, entries 1–4 in Table 1 establish that the quantum yields decrease with either the relative permittivity (ε) or the Dimroth–Reichardt parameter $E_T(30)$, both of which represent quantitative measures for the polarity of the solvent.[25] In fact, oxetane formation in the highly polar acetonitrile was completely suppressed ($\Phi = 0$). The electron donicity of the solvent is expressed in Table 1 in terms of either the Gutmann donor number[25] or the gas-phase ionization potential.[26] Entries 5–7 show that the quantum yield of oxetane formation decreased drastically with increasing electron donicity of the solvent as evaluated by the ionization potential. However, no clear correlation was obtained between the quantum yields of oxetane formation and Gutmann's donor numbers, which represent a different measure of the donor strength independent of its σ, π, or n-character.[25] Particularly noteworthy is the high quantum efficiency of $\Phi = 0.34$ obtainable in dioxane, a solvent of low polarity and relatively high donicity.

The presence of 0.1 M tetra-*n*-butylammonium hexafluorophosphate resulted in the quantum efficiencies which decreased by a factor of seven in dioxane (compare entries 4 and 8) and a factor of five in tetrahydrofuran (compare entries 3 and 9). Most strikingly, the photocoupling in tetrahydrofuran solution could be completely suppressed by the addition of rather small amounts (1 M) of inert salt (see entry 10).

II. Complex formation of chloranil with donor solvents

The unique dependence of the quantum yields in Table 1 on the solvent donicity, and in particular the outstanding solvent effect of dioxane, prompted our investigation of possible donor–acceptor interactions between chloranil and the solvent. We therefore carefully examined the changes in the absorption spectra of chloranil in dichloromethane upon incremental addition of the donor solvent. For example, the absorption band of chloranil (at λ_{max} = 294 nm) decreased significantly, and a new broad absorption at λ_{max} = 312 nm grew concomitantly with increasing molar fraction of dioxane in a dioxane–dichloromethane solvent mixture (see Fig. 1). The absorption changes were attributed to the formation of a donor/acceptor (EDA) complex[27] between chloranil and dioxane, the formation constant (K_{EDA}) and extinction coefficient (ε_{CT}) of which were evaluated by the Benesi–Hildebrand method[28] (see the Experimental section). Similar changes in the absorption spectra of chloranil were observed in solvents consisting of tetrahydrofuran–dichloromethane mixtures with increasing THF content; and the properties of the chloranil complexes with dioxane and tetrahydrofuran are listed in Table 2. For comparison, the corresponding data for EDA complexes of chloranil with aromatic donor solvents such as benzene, toluene, and *p*-xylene are also given in the table.[29] Although the values of K_{EDA} for the chloranil complexes were less than unity, the complexation of chloranil by donor solvents can strongly affect the efficiency of photocycloaddition to stilbene donors which are present in substantially lower concentrations relative to the neat (donor) solvent.

Table 2 Formation of EDA complexes of chloranil with donor solvents[a]

Solvent	λ_{max}[b]/nm	ε_s[c]/M^{-1} cm^{-1}	K_s[c]/M^{-1}
Dioxane	312	4360 ± 1500	0.05 ± 0.03
Tetrahydrofuran	312	5740 ± 1500	0.05 ± 0.02
Benzene[d]	340	2180	0.30
Toluene[d]	365	1920	0.50
p-Xylene[d]	415	1960	0.89

[a] Complex formation with dioxane and tetrahydrofuran measured in dichloromethane (as inert solvent). [b] By spectral subtraction. [c] By the Benesi–Hildebrand procedure (see ref. 28). [d] See ref. 29.

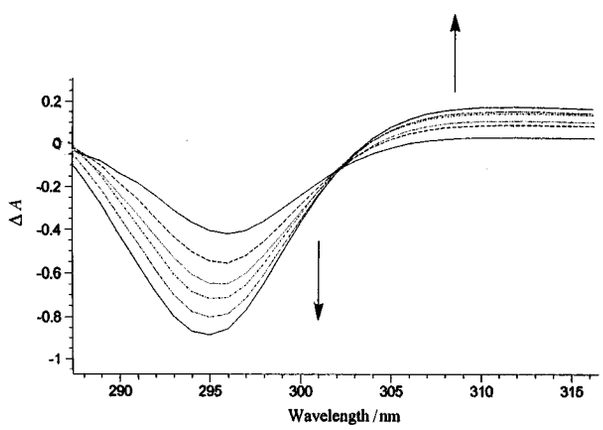

Fig. 1 Monotonic bleaching of the chloranil absorption (at 294 nm) and the growth of the charge-transfer absorption of the chloranil–dioxane complex (at 312 nm) upon the incremental addition (0.4, 0.8, 1.2, 1.8, 2.8 and 5.6 mL) of a 0.0001 M solution of chloranil in dioxane to an equimolar solution (1.5 mL) of chloranil in dichloromethane. [The difference spectra were obtained by digital subtraction of the spectrum of the original solution of chloranil in dichloromethane.]

III. Observation of radical ions upon laser excitation of chloranil in the presence of stilbene. Solvent and salt effects on the ion-pair dynamics

To study the solvent and salt effects on the formation and fate of the ion-radical intermediates in the chloranil–stilbene photocoupling reaction, photoexcited chloranil was generated by laser excitation (with a 10 ns pulse at 355 nm and a 200 fs pulse at 400 nm) in various solvents, and its subsequent quenching by stilbene was monitored by time-resolved spectroscopy on three distinctive (ps, ns, and μs) timescales as follows:

A. Formation of long-lived ion radicals in acetonitrile. We initially excited a solution of chloranil (0.004 M) and (*E*)-

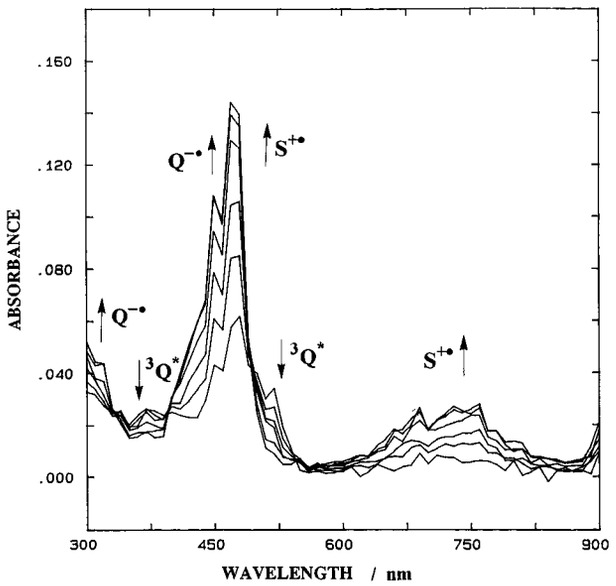

Fig. 2 Spectral changes at 370, 430, 500, 620, 800 and 1000 ns following the application of a 10 ns laser pulse at $\lambda_{exc} = 355$ nm to a solution of 0.0001 M stilbene and 0.004 M chloranil in acetonitrile showing the decay of triplet chloranil (^{3}Q*) at 370 and 510 nm and simultaneous growth of stilbene cation radical ($S^{+\bullet}$) at 480 and 760 nm and chloranil anion radical ($Q^{-\bullet}$) at 320 and 450 nm.

stilbene (0.0001 M) in acetonitrile with the 10 ns laser pulse of a Q-switched Nd:YAG laser at 355 nm; and the selective photoexcitation of chloranil resulted in the formation of its excited triplet state. As shown in Fig. 2, the chloranil triplet (with absorption bands centered at 370 and 510 nm)[14] decayed completely over the timespan of 1 μs. Concomitantly, the formation of stilbene cation radical ($S^{+\bullet}$ at 480 and 760 nm)[23] and chloranil anion radical ($Q^{-\bullet}$ at 320 and 450 nm)[22] was observed. The kinetics analysis of the triplet decay and the ion-radical formation resulted in identical first-order rate constants. The observed first-order rate constant of $k = 2.6 \times 10^6$ s^{-1} at a stilbene concentration of 10^{-4} M corresponded to a diffusion-controlled[30] second-order rate constant of $k_q = 2.6 \times 10^{10}$ M^{-1} s^{-1} for the electron-transfer quenching of triplet chloranil by stilbene according to eqn. (3).

$$^3Q^* + S \xrightarrow{k_q} Q^{-\bullet} - S^{+\bullet} \qquad (3)$$

Subsequently, the chloranil and stilbene ion radicals decayed to the spectral baseline on the μs timescale by second-order kinetics (not shown in the figure). It must be emphasized at this stage that ion-pair dynamics in acetonitrile occurred without any cycloaddition taking place, since no oxetane products (or any other photoproducts) were observed (see Table 1).

B. Formation of ion-radical pairs in dioxane. Laser irradiation at $\lambda_{exc} = 355$ nm of dioxane solutions (same as that described above for acetonitrile) also generated the triplet state of chloranil (^{3}**Q***) as the first observable intermediate upon application of a 10 ns laser pulse, but it decayed rapidly ($\tau \approx 250$ ns) to the spectral baseline without any signs of ion-radical formation. Since this result did not exclude the existence of very short-lived ($\tau < 10$ ns) ion-radical pairs (not detectable in a 10 ns laser experiment), the quenching of triplet chloranil in dioxane was repeated on the picosecond timescale by employing a much higher (0.1 M) stilbene concentration to ensure complete (diffusional) quenching within about 1 ns.[31] Since such concentrated stilbene solutions absorbed significantly at 355 nm, we employed a Ti:sapphire laser tuned to 406 nm to obviate any adventitious photoactivation of stilbene. Thus, the fast laser excitation of a solution of chloranil (0.008 M) and (*E*)-stilbene (0.1 M) in dioxane with a 200 fs pulse at 406 nm

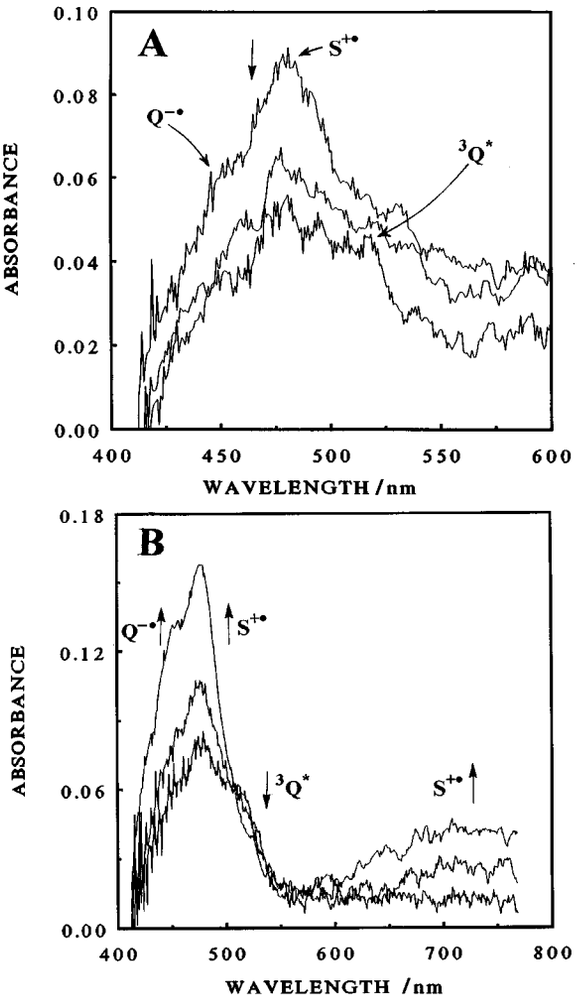

Fig. 3 Transient spectra obtained at (A) 0, 5 and 20 ps and (B) 100, 300 and 1600 ps upon the application of a 200 fs laser pulse at $\lambda_{exc} = 406$ nm to a solution of 0.1 M stilbene and 0.008 M chloranil in dioxane. Fig. 3A shows the fast decay of the [$S^{+\bullet}$, $Q^{-\bullet}$] ion pair generated by CT excitation of the chloranil–stilbene EDA complex. Fig. 3B shows the slower growth of stilbene cation radical (at 480 and 760 nm) and chloranil anion radical (at 450 nm) due to diffusional (electron-transfer) quenching of triplet chloranil (^{3}Q*, at 510 nm).

generated the spectral transient consisting of chloranil anion radical and (*E*)-stilbene cation radical at $\lambda_{max} = 450$ and 480 nm, respectively,[22,23] as shown in Fig. 3A. The subsequent decay of the transient absorptions was biphasic. *First*, both absorptions decayed rapidly to half of their original intensities within 20 ps, and a new spectrum evolved which clearly showed the 510 nm absorption of chloranil triplet (^{3}**Q***) in addition to some residual absorption of $S^{+\bullet}$ and $Q^{-\bullet}$ (see Fig. 3A). The kinetics profile of this fast initial decay is shown in the inset of Fig. 4, and the exponential fit of the data led to a single rate constant of $k_{fast} = 3.0 \times 10^{11}$ s^{-1}. Such fast rate constants for ion-radical decays are generally observed for back-electron transfer within contact ion-radical pairs,[32,33] and we ascribe these initial short-lived transient absorptions to the singlet ion-radical pair ^{1}[$S^{+\bullet}$, $Q^{-\bullet}$],[34] which was directly generated by laser excitation of the charge-transfer absorptions of the electron donor-acceptor (EDA) complex of chloranil with stilbene. [Note that there was significant EDA complex formation at 0.1 M stilbene concentration.] *Second*, the residual transient absorptions exhibited further changes on a much slower timescale. Thus, Fig. 3B shows the absorption bands at 450 and 480 nm, as well as that at 760 nm growing again (following the initial fast decay) over a timespan of about 1.5 ns. Concomitantly, the absorption of triplet chloranil at 510 nm decayed at the same rate. Fig. 4 shows that the kinetic traces for this slow

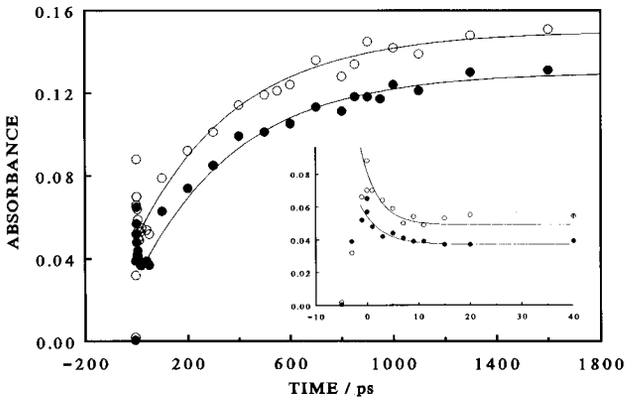

Fig. 4 Ultrafast decay followed by the slow formation of the ion-radical pair [$S^{+\bullet}$, $Q^{-\bullet}$] monitored at 450 (●) and 480 (○) nm upon the 200 fs laser excitation of a solution of 0.1 M stilbene and 0.008 M chloranil in dioxane at 406 nm. The inset shows a magnified view of the initial ultrafast decay. Both the decay and formation traces are fitted to first-order kinetics (solid lines) with rate constants of $k_{fast} = 3 \times 10^{11}$ s^{-1} and $k_{slow} = 2.5 \times 10^{9}$ s^{-1}.

growth could be fitted to first-order kinetics with a rate constant of $k_{slow} = 2.5 \times 10^{9}$ s^{-1}. The slow decay of ^{3}**Q*** and the concomitant formation of $\mathbf{Q}^{-\bullet}$ and $\mathbf{S}^{+\bullet}$ were assigned to the diffusional electron-transfer quenching of triplet chloranil by stilbene, and the bimolecular quenching rate constant was calculated as $k_{bim} = k_{slow}/[\mathbf{S}] = 2.5 \times 10^{10}$ M^{-1} s^{-1}. Thus, these results show that excited triplet chloranil was quenched by stilbene both in acetonitrile and in dioxane solution at diffusion-limited rates[31] to afford chloranil anion and (*E*)-stilbene cation radicals. The ion-radical absorptions in acetonitrile (see Fig. 2), which persisted over tens of microseconds were ascribed to the free, solvated ion radicals, which are generally observable in polar solvents as a result of rapid ion-pair separation.[21c] By contrast, the ion-radical absorptions in dioxane decayed much faster with a lifetime of about 5 ns. Since ion pairing is favored in less polar solvents, we ascribe the 5 ns (ion-radical) absorptions in dioxane to the *triplet* ion-radical pairs.

C. The effects of added salt on the ion-pair dynamics in tetrahydrofuran. Laser experiments in tetrahydrofuran were carried out to investigate the salt effect on the electron-transfer kinetics. In the absence of salt, the laser excitation of a solution of chloranil (0.004 M) and stilbene (0.001 M) in tetrahydrofuran with a 10 ns laser pulse at 355 nm generated first the triplet chloranil which decayed very rapidly with a lifetime of $\tau = 350$ ns. Concomitantly, the formation of chloranil semiquinone radical (**QH**$^\bullet$ or the hydrochloranil radical) was observed with its diagnostic (narrow) absorption bands at 360 and 435 nm.[35] In other words, the triplet chloranil mainly abstracted hydrogen atoms from tetrahydrofuran,[36] and evidently only a small portion ($\Phi = 0.05$ in Table 1) reacted with stilbene to yield the oxetane product.

Upon the addition of salt (0.1 M tetra-*n*-butylammonium hexafluorophosphate), the transient absorption spectra obtained upon 355 nm laser excitation of the same tetrahydrofuran solution exhibited absorption bands very similar to those observed in acetonitrile solution (compare Fig. 2 and 5). Thus, the initial absorption of triplet chloranil at 510 nm decayed with a rate constant of $k = 2.6 \times 10^{6}$ s^{-1}, and chloranil anion radical (450 nm)[22] and stilbene cation radical (480 and 760 nm)[23] were simultaneously observed. Under these conditions, no hydrochloranil radicals were observed,[36b] but long-lived (μs) ion radicals were generated *via* diffusion-controlled ($k_{bim} = 2.6 \times 10^{10}$ M^{-1} s^{-1})[30] electron-transfer quenching of *triplet* chloranil by stilbene. However, a close inspection of the transient spectra in acetonitrile and tetrahydrofuran containing 0.1 M salt revealed that the yield of ion radicals produced in THF

Table 3 Photocoupling of (*Z*)-stilbene with chloranil[a]

Time/ min	[Chloranil][b]/ mol L^{-1}	[(*Z*)-stilbene][b]/ mol L^{-1}	[(*E*)-stilbene][b]/ mol L^{-1}	[Spiro-oxetane][b]/ mol L^{-1}
142	0.0470	0.0409	0.0059	0.0024
191	0.0461	0.0379	0.0076	0.0032
245	0.0457	0.0364	0.0091	0.0041
303	0.0450	0.0323	0.0103	0.0048
338	0.0437	0.0307	0.0108	0.0054
384	0.0424	0.0288	0.0120	0.0061
424	0.0423	0.0282	0.0131	0.0072
462	0.0418	0.0262	0.0134	0.0077

[a] In dioxane solution of 0.05 M chloranil and 0.05 M (*Z*)-stilbene irradiated at $\lambda_{exc} = 436$ nm. [b] By HPLC analysis.

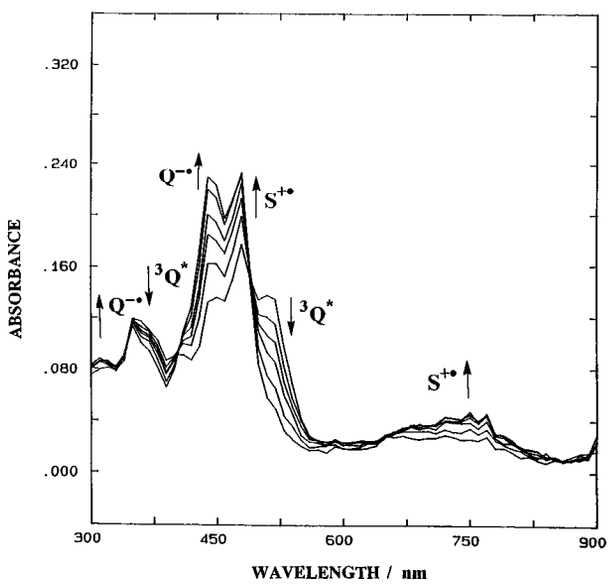

Fig. 5 Transient spectra obtained at 330, 400, 470, 540, 680 and 890 ns following the application of a 10 ns laser pulse at $\lambda_{exc} = 355$ nm to a solution of 0.0001 M stilbene and 0.004 M chloranil in tetrahydrofuran containing 0.1 M tetrabutylammonium hexafluorophosphate salt showing the decay of triplet chloranil (^{3}Q*) at 370 and 510 nm and simultaneous growth of stilbene cation radical ($\mathbf{S}^{+\bullet}$) at 480 and 760 nm and chloranil anion radical ($\mathbf{Q}^{-\bullet}$) at 320 and 450 nm.

with salt amounted to only half that observed in acetonitrile. [Compare the relative absorbances of stilbene cation radical at 480 nm and chloranil triplet at 510 nm in Fig. 2 and 5].

IV. Photocoupling of chloranil to (*Z*)-stilbene

The Paterno–Büchi coupling of chloranil and stilbene selectively yielded *trans*-oxetane **1** in eqn. (1) even when pure (*Z*)-stilbene was used as reactant.[1] Thus, the question arose at which stage during the reaction (*Z*)-stilbene was converted to the *trans* isomer. Accordingly, a kinetic study of the photocoupling of chloranil to (*Z*)-stilbene was carried as follows. An equimolar solution of chloranil and (*Z*)-stilbene in dioxane was irradiated at $\lambda_{exc} = 436$ nm, and the simultaneous disappearance of chloranil and (*Z*)-stilbene [as well as the appearance of *trans*-spirooxetane and (*E*)-stilbene] was periodically monitored by HPLC analysis (see Experimental section). Table 3 shows the change in concentration of all reactants and products over time. From the slope of the linear ($R > 0.97$) concentration–time plots *versus* the intensity of the light source (determined by ferrioxalate actinometry),[24] the quantum yields for the consumption of chloranil and [*Z*)-stilbene [and for the production of *trans*-spirooxetane and (*E*)-stilbene] were determined to be 0.18, 0.48, 0.18 and 0.27 (± 0.01), respectively. Thus, the consumption of chloranil and the production of spirooxetane occurred at the same rate and quantum efficiency. Furthermore,

the consumption of (*Z*)-stilbene occurred with a quantum efficiency equal to the sum of the (*E*)-stilbene and *trans*-spirooxetane efficiencies.

Discussion

The variation of solvent properties and the presence of inert salt result in two kinds of effects on the Paterno–Büchi coupling of stilbene and chloranil in eqn. (1). First, the *quantum yield* for oxetane formation (as determined by steady-state irradiation and chemical actinometry) is extremely sensitive to the polarity and donicity of the solvent and to the deliberate addition of salt. Second, the *decay pathway* of the critical ion-radical intermediates (as observed by time-resolved absorption spectroscopy) strongly depends on the solvent environment including the presence of added salt. To relate these independent observations, let us now analyze the solvent and salt effects on the various (individual) steps in the photocoupling mechanism which is based on an initial electron transfer from the stilbene donor to the quinone acceptor.[2]

I. Solvent-donicity effects on the formation of the quinone–stilbene encounter complex

Previous studies on bimolecular (diffusional) electron transfer from various arene donors to photoactivated quinone establish the encounter complex to be the primary reactive intermediate prior to electron transfer.[14] Strong electronic coupling between the donor and the acceptor moiety in the encounter complex [as revealed by its intense (near IR) charge-transfer absorptions][14] effects a sizable predisposition to electron transfer, and it results in electron transfer at fast rates and with high efficiency. In the same way, we envisage stilbene to be involved in the preequilibrium association with the photoactivated chloranil, [eqn. (4)].

$$^3Q^* + S \overset{K_{EDA}}{\rightleftharpoons} {}^3[S,Q^*] \qquad (4)$$

However, solvent molecules of high electron donicity interfere with the formation of the initial chloranil–stilbene encounter complex, and the overall quantum efficiency of oxetane formation is affected as follows. Solvents of high π-donicity such as benzene, toluene, or *p*-xylene (see entries 5–7 in Table 1) strongly compete with the stilbene donor (which is present in substantially lower concentration), to form the arene–quinone encounter complex.[29] Table 2 demonstrates that complex formation with chloranil (even in its ground state) increases with increasing π-donor strength of the solvent. In fact, the strong complexation of chloranil by (neat) *p*-xylene leads to almost complete removal of stilbene from the primary solvation shell of the photoactivated quinone; and it thus reduces the quantum efficiency of photocoupling substantially to $\Phi = 0.01$ in Table 1.

In contrast, the complexation of quinone by dioxane (see Fig. 1 and Table 2) does not interfere with the formation of the critical chloranil–stilbene encounter complexes. On the contrary, the best photocoupling efficiency is obtained in dioxane (see Table 1). This suggests that the electron-acceptor properties of quinone are even enhanced, and electron transfer from the stilbene donor is very efficient. However, the unique solvent effect of dioxane on the photocoupling efficiency cannot be explained solely by a consideration of solvent complexation. Thus, comparison with tetrahydrofuran [a solvent of higher (Gutmann) donicity but also higher polarity] shows clearly that even solvents of comparable complexation capabilities (see Table 2) can effect quite different photocoupling efficiencies (see Table 1) owing to polarity differences discussed in the following section.

II. Solvent-polarity effects on the decay pathway of the ion-radical intermediates

Electron-transfer quenching of photoactivated (triplet) quinone leads [*via* the intermediate encounter complexes in eqn. (4)] to triplet ion-radical pairs[14] [eqn. (5)].

$$^3[S,Q^*] \xrightarrow{k_{ET}} {}^3[S^{+\bullet},Q^{-\bullet}] \qquad (5)$$

The various pathways for the subsequent decay of the triplet ion-radical pair in eqn. (5) are delineated in Scheme 1.

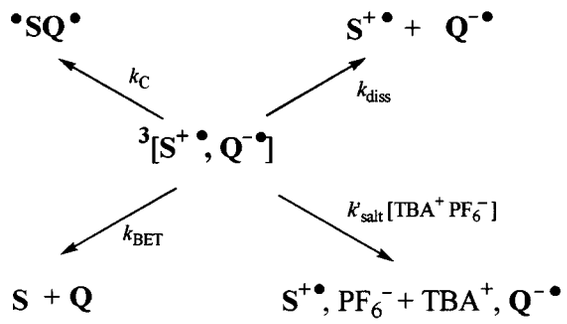

Scheme 1

The polarity of the solvent environment shows its strongest effect in controlling the predominant pathway of the triplet ion-radical pair as follows: With increasing polarity of the solvent, the triplet ion-radical pair [$S^{+\bullet}$, $Q^{-\bullet}$] in Scheme 1 suffers an increasingly rapid dissociation (k_{diss}) into free (solvated) ion radicals.[21c,37] In fact, free-ion yields close to unity have been reported in highly polar acetonitrile as the result of electron-transfer (ET) quenching of triplet quinones by various aromatic donors.[14,16] Fig. 2 presents the same scenario for ET quenching of chloranil by stilbene, *i.e.* long-lived (μs) transient absorptions are observed in *acetonitrile*, which are ascribed to the free (solvated) $Q^{-\bullet}$ and $S^{+\bullet}$ ion radicals. Most importantly, no photocoupling of chloranil and stilbene to the oxetane adduct is obtained under these conditions, and we come to the following conclusion: Coupling (k_C in Scheme 1) of the $Q^{-\bullet}$ and the $S^{+\bullet}$ ion radicals to form the triplet 1,4-biradical ($^{\bullet}SQ^{\bullet}$) occurs exclusively from the triplet ion-pair state, whereas the collision of the free ion radicals results in a second-order decay by back electron transfer to restore the starting material. Thus, the dissociation of the ion pair (k_{diss} in Scheme 1) into free ions reduces the oxetane yields. In fact, the quantum yield of zero for oxetane formation in acetonitrile reveals that ion dissociation completely outruns the coupling process ($k_{diss} \gg k_C$) in this highly polar environment.[38a] On the basis of reaction Scheme 1, the quantum yield of oxetane formation in acetonitrile is $\Phi = k_C/(k_C + k_{diss})$ [note that $k_{salt} = 0$ and $k_{BET} \ll k_{diss}$].[39] Thus, by taking $k_{diss} \cong 1 \times 10^9$ s^{-1} in acetonitrile[21c,37] and $\Phi = 0 \pm 0.01$, we calculate the coupling rate constants to be $k_C \leq 1 \times 10^7$ s^{-1}.[38b]

In contrast, the ion-radical absorptions in *dioxane* (see Fig. 3) which decay within 5 ns are ascribed to the triplet ion pair. As such, free (solvated) ion radicals (with μs lifetimes and second-order decay kinetics) are not observed in this nonpolar environment. Evidently, ion dissociation does not compete with the coupling process under these conditions, and the quantum yield for oxetane formation is solely limited by the competition between back-electron transfer (k_{BET}) and coupling (k_C), *i.e.* $\Phi = k_C/(k_C + k_{BET})$. Accordingly, the quantum yield of $\Phi = 0.34$ in dioxane reveals the relative ratio of coupling and back electron transfer rates to be approximately 1 : 2. Finally for solvents of intermediate polarity, the quantum yield for oxetane formation is determined by the relative rate of coupling as compared to back-electron transfer and ionic dissociation, both of which depend on the solvent polarity.

III. Salt effects on the ion-pair dynamics

The presence of added (inert) salt affects the decay pathway of

the ion-radical pair in a manner similar to that observed in highly polar solvents. Thus, ion-radical pairs are known to interact with inert salt by ion exchange,[40] which is tantamount to the separation of the chloranil anion and the stilbene cation (see Scheme 1). As a result, the separated ion radicals are observed (as illustrated in Fig. 5) with lifetimes comparable to those in acetonitrile. Moreover, the salt-induced free ion radicals in Fig. 5 do not undergo coupling to the oxetane—as evidenced by the decrease in oxetane yields with increasing salt concentration (see Table 1). If the ion exchange follows second-order kinetics (to a first approximation), its observed pseudo first-order rate constant will depend linearly on the salt concentration, *i.e.* $k_{salt} = k'_{salt}$ [salt]. Accordingly, the oxetane yields (Φ) will vary with the reciprocal of the salt concentration. From the decrease of Φ as a function of the salt concentration (in Table 1), we calculate the second-order rate constant for ion exchange in dioxane to be 170 times faster than the coupling rate constant so that $k'_{salt} \cong 2 \times 10^9$ M^{-1} s^{-1} for $k_C \cong 1 \times 10^7$ s^{-1} (*vide supra*).[41] Thus, the interception of the ion-radical pair by salt occurs at almost diffusion-limited rates,[31] and consequently salt concentrations of 0.1 M are sufficient to reduce the quantum yield of oxetane formation significantly (see Table 1). In fact, oxetane formation can even be completely suppressed at relatively low salt concentrations of ~1 M in tetrahydrofuran (see Table 1).

IV. *cis*→*trans* Isomerization in the Paterno–Büchi coupling of (*Z*)-stilbene and quinone

Photocoupling of stilbene and quinone yields the same *trans*-oxetane adduct regardless of the geometrical (*cis* or *trans*) configuration of the stilbene.[1] Since (*Z*)-stilbene undergoes efficient *cis*→*trans* isomerization in the presence of electron-transfer sensitizers,[42] the question arises as to whether (a) (*Z*)-stilbene in its cation-radical state isomerizes to the *trans* isomer before it couples with the chloranil anion radical, (b) *cis*→*trans* isomerization and coupling are independent (parallel) reactions, or (c) processes (a) and (b) are competitive. A definitive answer to this question is based on the quantitative comparison of the quantum yields derived from the kinetic data in Table 3 with the quantum yield of oxetane formation from pure (*E*)-stilbene ($\Phi_{ox,E} = 0.34$) in dioxane as follows: First, we note that the quantum yield of oxetane formation from (*Z*)-stilbene ($\Phi_{ox,Z} = 0.18$, which is directly derived from the data in Table 3) is substantially lower than that from (*E*)-stilbene (*vide supra*). If *trans*-oxetane is only formed by coupling of (*E*)-stilbene cation radical with chloranil anion radical (process a), the overall yield of oxetane formation from (*Z*)-stilbene will be determined by the product of Φ_Z and $\Phi_{ox,E}$, where $\Phi_Z = 0.48$ is the quantum yield of (*Z*)-stilbene consumption (which equals the yield of (*E*)-stilbene cation-radical formed). This consecutive mechanism thus yields a calculated quantum yield of $\Phi^c_{ox,Z} = \Phi_Z \times \Phi_{ox,E} = 0.16$, which is in close agreement with the experimental value of $\Phi_{ox,Z} = 0.18$. Any significant contribution from a direct pathway from (*Z*)-stilbene cation radical to the oxetane (process b or c) would lead to a noticeable difference between experimental and calculated quantum yield of oxetane formation from (*Z*)-stilbene. As such, we conclude that the *trans*-oxetane is mostly formed by coupling of (*E*)-stilbene cation radical (process a); and the direct coupling of (*Z*)-stilbene cation radical to afford the *trans*-oxetane must be negligible.

Summary and conclusions

The quantum yield of oxetane formation in the Paterno–Büchi coupling of chloranil and stilbene depends strongly on the polarity and donicity of the solvent. Deliberate addition of inert salt in dioxane or tetrahydrofuran significantly reduces the quantum yield or it can even suppress the coupling reaction completely. Time-resolved absorption measurements on the ps/ns/μs timescales reveal the ion-radical pair [$S^{+\bullet}$, $Q^{-\bullet}$] to be the critical intermediate, and thus confirm the electron-transfer mechanism for chloranil–stilbene photocoupling.[2] The competition between the various reaction pathways for the decay of the ion-radical pair in Scheme 1 is controlled by solvent and salt effects, and can thus be directly related to the solvent and salt effects on the quantum yields of oxetane formation. The quantitative analysis of the kinetic data and the quantum yield in acetonitrile lead to a rate constant $k_C \leq 1 \times 10^7$ s^{-1} for the (rate determining) coupling of the triplet ion-radical pair to the triplet 1,4-biradical, which then cyclizes to the final oxetane product. Moreover, *trans*-oxetane formation from (*Z*)-stilbene proceeds *via* a *cis*→*trans* isomerization of the (*Z*)-stilbene cation radical prior to the coupling step. Thus, all variations in the quantum efficiency of the Paterno–Büchi coupling of quinone and stilbene owing to solvent and salt effects and the stilbene configuration are readily explained by the differences in the microdynamics of the critical ion-radical pair from stilbene and the quinone.

Experimental

Materials and methods

Tetrachloro-*p*-benzoquinone (chloranil, Aldrich) was sublimed *in vacuo* and recrystallized from benzene. (*E*)- and (*Z*)-stilbene from Aldrich were used as received. All solvents were purified following standard procedures.[43] ^{1}H NMR spectra were recorded in $CDCl_3$ on a General Electric QE-300 spectrometer, and the chemical shifts are reported in ppm units downfield from internal tetramethylsilane. UV–vis and IR spectra were recorded on a Hewlett-Packard 8453 diode-array spectrophotometer and a Nicolet 10 DX Fourier-transfer spectrometer, respectively. HPLC analyses were performed on an LDC Analytical Instrument (SM 3100) equipped with a Hypersil BDS C18 reverse-phase column (20 cm) with methanol–water mixtures as eluent.

Photoinduced coupling of chloranil and stilbene

Preparative photolysis. A solution of chloranil (1 mmol, 0.05 M) and stilbene (2 mmol, 0.1 M) in benzene was irradiated under argon with a focused beam from a medium-pressure mercury lamp (500 W) passed through an aqueous IR filter and an ESCO 370 nm cut-off filter. This ensured that only the quinone (and not the stilbene) absorbed the actinic light. The photoreaction was carried out until HPLC analysis showed the complete consumption of chloranil. The solvent was evaporated and the crude product washed with petroleum ether and recrystallized from chloroform–petroleum ether. The *trans*-spirooxetane **1** [see eqn. (1)] was isolated in 86% yield, and its characteristic physical data are as follows: 5,6,8,9-Tetrachloro-2,3-diphenyl-1-oxaspiro[3,5]nona-5,8-dien-7-one, **1**: mp 150–151 °C (decomp.) (lit. 150 °C)[1]; IR (cm^{-1}): 1686, 1606, 1575, 1497, 1127, 1102, 968, 826, 773, 753, 742, 733, 723, 698, 682, 651, 551; ^{1}H NMR ($CDCl_3$): δ, 4.98 (d, 1H, J 8.7), 6.72 (d, 1H, J 9.0), 7.30–7.60 (m, 10H).

Determination of quantum yields of oxetane formation. The quantum yields were measured with the aid of a medium-pressure (500 W) mercury lamp focused through an aqueous IR filter followed by an aqueous $NaNO_2$–$CuSO_4$ solution filter with a narrow-band pass at 440 ± 30 nm. The intensity of the lamp was determined with a freshly prepared potassium ferrioxalate actinometer solution[24] in a 1 cm cuvette fitted with a Schlenk adapter. The absorbance at 436 nm of a solution of chloranil (0.05 M) and (*E*)-stilbene (0.01 M) in all solvents remained above 1.5 throughout the irradiation, and thus no correction for transmitted light was necessary. A 20 μL aliquot was taken, diluted with 5 mL of methanol, and the contents quantified by HPLC using biphenyl as an internal standard.

The quantum yields for oxetane formation in various solvents are listed in Table 1.

Formation constants of solvent complexes with chloranil

In a typical procedure, a 1.5 mL aliquot of a 0.1 mM solution of chloranil in dichloromethane was transferred to a 1 cm quartz cuvette. An equimolar (0.1 mM) solution of chloranil in a donor solvent (dioxane or tetrahydrofuran) was added incrementally. The absorption changes were measured at the spectral maxima as well as at other wavelengths close to the absorption maxima. From the growth of the new absorption band at 312 nm with increasing molar fraction of either dioxane or tetrahydrofuran, the equilibrium constants (K_s) for the formation of the chloranil–solvent complexes were determined by the application of the Benesi–Hildebrand method.[28] Thus, the plot of $[\mathbf{Q}]/A_s$ *vs.* $[\text{solvent}]^{-1}$ was linear with a correlation coefficient $R > 0.97$, and the extinction coefficients (ε_s) and the formation constants (K_s) were calculated from the intercept and the slope.[28] The K_s values were substantially smaller for oxygen-donor solvents relative to those evaluated for aromatic solvents, such as benzene, toluene, and *p*-xylene reported earlier[29] (see Table 2).

Photocoupling of (*Z*)-stilbene with chloranil

An equimolar solution of chloranil and (*Z*)-stilbene in dioxane was irradiated at $\lambda_{exc} = 436$ nm, and the simultaneous disappearance of chloranil and (*Z*)-stilbene [as well as the appearance of *trans*-spirooxetane and (*E*)-stilbene] was periodically monitored by HPLC analysis (up to 8 h). This kinetics study was carried out with the aid of a medium-pressure (500 W) mercury lamp that was focused through an aqueous IR filter followed by an aqueous $NaNO_2$–$CuSO_4$ solution filter (440 ± 30 nm). The 1 cm cuvette fitted with a Schlenk adapter was filled with a solution of chloranil (0.05 M) and (*Z*)-stilbene (0.05 M) in 3 mL dioxane under argon. At various times during the irradiation, a 20 μL aliquot was extracted and diluted with 5 mL of methanol. The four components [chloranil, (*Z*)-stilbene, (*E*)-stilbene and spirooxetane] of the reaction mixture were quantified by HPLC with biphenyl as an internal standard. The overall conversion of the reactants was kept below 15% in order to avoid the competitive quenching of excited chloranil by (*E*)-stilbene formed during the photoreaction. Table 3 shows the change in concentration of all reactants and products over time, and from the slope of the linear ($R > 0.97$) concentration–time plots *versus* the intensity of the light source (determined by ferrioxalate actinometry[24]), the quantum yields for the consumption of chloranil and (*Z*)-stilbene [and for the production of *trans*-spirooxetane and (*E*)-stilbene] were determined to be 0.18, 0.48, 0.18 and 0.27, respectively. Thus, the consumption of chloranil and the production of spirooxetane occurred at the same rate and quantum efficiency. Furthermore, the consumption of (*Z*)-stilbene occurred with a quantum efficiency equal to the sum of (*E*)-stilbene and *trans*-spirooxetane efficiencies.

Time-resolved absorption spectra from photoexcitation of chloranil with stilbene

Laser excitation of chloranil at $\lambda_{exc} = 355$ nm. The nanosecond/microsecond time-resolved absorption measurements were carried out with a kinetic spectrometer including a Quantel (YG580-10) Q-switched Nd^{3+}:YAG laser (10 ns pulsewidth).[44] The third (355 nm) harmonic output was used for the excitation of chloranil. The solutions of chloranil and (*E*)-stilbenes were prepared under an argon atmostphere in a 1 cm cuvette fitted with a Schlenk adapter. The concentrations of the components were adjusted for absorbances in the range 0.5–0.8 at the excitation wavelength of $\lambda_{exc} = 355$ nm.

Laser excitation at 406 nm. To monitor the quenching of photoexcited quinone by stilbene in dioxane on the picosecond timescale, chloranil was excited at 406 nm (to avoid the unintentional photoexcitation of stilbene). The excitation at 406 nm was achieved with a Ti:sapphire laser system consisting of a Photonics Industries Ti:sapphire oscillator coupled to a Coherent Innova 310 argon-ion laser and two consecutive Photonics Industries Ti:sapphire amplifiers pumped by a Continuum Surelite I Nd:YAG laser at 10 Hz.[45]

Acknowledgements

We thank the R. A. Welch Foundation and the National Science Foundation for financial support.

References

1 J.-H. Xu, L.-C. Wang, J.-W. Xu, B.-Z. Yan and H.-C. Yuan, *J. Chem. Soc., Perkin Trans. 1*, 1994, 571.
2 D. Sun, S. M. Hubig and J. K. Kochi, *J. Org. Chem.*, in the press.
3 E. Paterno and G. Chieffi, *Gazz. Chim. Ital.*, 1909, **39**, 341; G. Büchi, C. G. Inman and E. S. Lipinsky, *J. Am. Chem. Soc.*, 1954, **76**, 4327.
4 Spectroscopic studies on various Paterno–Büchi couplings have revealed several reactive intermediates including exciplexes,[5,6] ion-radical pairs,[6–10] and 1,4 biradicals.[8–12]
5 R. A. Caldwell, D. C. Hrncir, T. Muñoz, Jr. and D. J. Unett, *J. Am. Chem. Soc.*, 1996, **118**, 8741; R. A. Caldwell, G. W. Sovocool and R. P. Gajewski, *J. Am. Chem. Soc.*, 1973, **95**, 2549; N. E. Schore and N. J. Turro, *J. Am. Chem. Soc.*, 1975, **97**, 2482.
6 S. Hu and D. C. Neckers, *J. Org. Chem.*, 1997, **62**, 6820.
7 J. Gersdorf, J. Mattay and H. Görner, *J. Am. Chem. Soc.*, 1987, **109**, 1203.
8 S. C. Freilich and K. S. Peters, *J. Am. Chem. Soc.*, 1985, **107**, 3819; *J. Am. Chem. Soc.*, 1981, **103**, 6255.
9 A. G. Griesbeck, H. Mauder and S. Stadtmüller, *Acc. Chem. Res.*, 1994, **27**, 70.
10 G. Eckert and M. Goez, *J. Am. Chem. Soc.*, 1994, **116**, 11999.
11 D. I. Schuster, G. Lem and N. A. Kaprinidis, *Chem. Rev.*, 1993, **93**, 3.
12 S. Hu and D. C. Neckers, *J. Org. Chem.*, 1997, **62**, 564.
13 For reviews, see: G. Jones II, in *Organic Photochemistry*, ed. A. Padwa, Dekker, New York, 1981, vol. 5, p. 1; A. G. Griesbeck, in *CRC Handbook of Organic Photochemistry and Photobiology*, ed. W. M. Horspool and P.-S. Song, CRC Press, Boca Raton, FL, 1995, p. 522.
14 R. Rathore, S. M. Hubig and J. K. Kochi, *J. Am. Chem. Soc.*, 1997, **119**, 11468, and references therein.
15 E. Bosch, S. M. Hubig and J. K. Kochi, *J. Am. Chem. Soc.*, 1998, **120**, 386.
16 R. Gschwind and E. Haselbach, *Helv. Chim. Acta*, 1979, **62**, 941.
17 S. M. Hubig, T. M. Bockman and J. K. Kochi, *J. Am. Chem. Soc.*, 1997, **119**, 2926.
18 The reduction potential of the triplet quinone is $E^*_{red} = 2.15$ V *vs.* SCE. See ref. 14.
19 The oxidation (peak) potential of stilbene is $E^{P}_{ox} \cong 1.56$ V *vs.* SCE. See ref 23.
20 The triplet ion-radical pair in eqn. (2) then follows various reaction pathways including back-electron transfer,[21a,b] ion dissociation,[21c] and the critical coupling to the triplet 1,4-biradical[2] which subsequently undergoes ring closure to form the final oxetane product.[8–12]
21 (*a*) K. S. Peters, *Adv. Electron Transfer Chem.*, 1994, **4**, 27; (*b*) M. A. Fox, *Adv. Photochem.*, 1986, **13**, 237; (*c*) H. Knibbe, D. Rehm and A. Weller, *Ber. Bunsenges. Phys. Chem.*, 1968, **72**, 257.
22 The chloranil anion radical absorbs at $\lambda_{max} = 450$ nm and $\lambda_{max} = 320$ nm. See J. J. André and G. Weill, *Mol. Phys.*, 1968, **15**, 97.
23 The stilbene cation radical absorbs at $\lambda_{max} = 480$ and 760 nm. See: F. D. Lewis, A. M. Bedell, R. E. Dykstra, J. E. Elbert, I. R. Gould and S. Farid, *J. Am. Chem. Soc.*, 1990, **112**, 8055; T. Shida, *Electronic Absorption Spectra of Radical Ions*, Elsevier, New York, 1988, p. 112.
24 C. G. Hatchard and C. A. Parker, *Proc. R. Soc. London, Ser. A*, 1956, **235**, 518. See also: J. G. Calvert and J. N. Pitts, Jr., *Photochemistry*, Wiley, New York, 1996, p. 786.
25 C. Reichardt, *Solvent Effects in Organic Chemistry*, Verlag Chemie, New York, 1979.
26 R. C. Weast, *CRC Handbook of Chemistry and Physics*, 53rd edn., CRC Press, Boca Raton, FL, 1975, p. E73.
27 D. Bryce-Smith, B. F. Connett and A. Gilbert, *J. Chem. Soc. (B)*, 1968, 816; M. A. Slifkin, *Spectrochim. Acta, Part A*, 1969, **25**, 1037.

28 H. Benesi and J. H. Hildebrand, *J. Am. Chem. Soc.*, 1949, **71**, 2703; W. B. Person, *J. Am. Chem. Soc.*, 1965, **87**, 167.
29 J. N. Murrell, *J. Am. Chem. Soc.*, 1954, **81**, 5037.
30 J. W. Moore and R. G. Pearson, *Kinetics and Mechanism*, 3rd edn., Wiley, New York, 1981, p. 239.
31 Diffusion-controlled reactions occur with second-order rate constants of ~10^{10} M^{-1} s^{-1}. See ref. 30.
32 T. Asahi and N. Mataga, *J. Phys. Chem.*, 1989, **93**, 6575; 1991, **95**, 1956.
33 E. F. Hilinki, J. M. Masnovi, J. K. Kochi and P. M. Rentzepis, *J. Am. Chem. Soc.*, 1984, **106**, 8071.
34 S. Ojima, H. Miyasaka and N. Mataga, *J. Phys. Chem.*, 1990, **94**, 4147.
35 H. Kobashi, M.-A. Funabashi, T. Kondo, T. Morita, T. Okada and N. Mataga, *Bull. Chem. Soc. Jpn.*, 1984, **57**, 3557; H. Kobashi, T. Okada and N. Mataga, *Bull. Chem. Soc. Jpn.*, 1986, **59**, 1975; G. Jones II, W. A. Haney and X. T. Phan, *J. Am. Chem. Soc.*, 1988, **110**, 1922.
36 (*a*) The rate constant for H-atom abstraction was determined as $k_H = 2.9 \times 10^6$ s^{-1}. (*b*) It is not clear at this stage why the hydrogen abstraction is suppressed in the presence of high amounts of inert salt.
37 S. Ojima, H. Miyasaka and N. Mataga, *J. Phys. Chem.*, 1990, **94**, 7534.
38 (*a*) The coupling (k_C) of chloranil anion radical and stilbene cation radical to the 1,4-biradical intermediate represents the first (rate-determining) step toward oxetane formation by analogy with the biradical intermediates observed in the Paterno–Büchi coupling of benzoquinone and styrene. See: K. Maruyama, T. Otsuki and S. Tai, *J. Org. Chem.*, 1985, **50**, 52; K. Maruyama and H. Imahori, *J. Org. Chem.*, 1989, **54**, 2692. Note that in our study no further transient intermediates have been detected upon the decay of the ion-radical pairs. (*b*) The coupling rate constant of $k_C \leq 10^7$ s^{-1} in highly polar acetonitrile is substantially slower than that in (nonpolar) dioxane solution ($k_C \approx 10^8$ s^{-1}),[2] which is mainly due to the different solvation (and stabilization) of the ion-radical pairs in the two solvents. [Note also that the rate constant in dioxane solution was derived by a different method, *viz.* the quantitative evaluation of the competition between back electron transfer and coupling, since no dissociation of the ion pairs was observed.][2]
39 Free-ion yields close to unity imply that the dissociation rates are orders of magnitude faster than back electron transfer.[14,16]
40 S. M. Hubig, W. Jung and J. K. Kochi, *J. Org. Chem.*, 1994, **59**, 6233; T. Yabe and J. K. Kochi, *J. Am. Chem. Soc.*, 1992, **114**, 4491.
41 The quantum yield for oxetane formation is determined by the competition of all the decay pathways in Scheme 1, *i.e.* $\Phi = k_C/(k_C + k_{BET} + k_{diss} + k'_{salt}[salt])$. By taking $k'_{salt}[salt] \gg k_{BET}$ or k_{diss}, the quantum yield reduces to: $\Phi = k_C/(k_C + k'_{salt}[salt])$. Thus, the difference in Φ for [salt] = 0 and [salt] = 0.1 M in Table 1 (entries 4 and 8) leads to $k'_{salt} = 170 \times k_C$.
42 F. D. Lewis, J. R. Petisce, J. D. Oxman and M. J. Nepras, *J. Am. Chem. Soc.*, 1985, **107**, 203; Y. Kuriyama, H. Sakuragi, K. Tokumaru, Y. Yoshida and S. Tagawa, *Bull. Chem. Soc. Jpn.*, 1993, **66**, 1852; A. Corma, V. Fornés, H. Garcia, M. A. Miranda, J. Primo and M. Sabater, *J. Am. Chem. Soc.*, 1994, **116**, 2276.
43 D. D. Perrin, W. L. F. Armarego and D. R. Perrin, *Purification of Laboratory Chemicals*, 2nd edn., Pergamon, New York, 1980.
44 T. M. Bockman and J. K. Kochi, *J. Chem. Soc., Perkin Trans. 2*, 1996, 1633.
45 S. M. Hubig, T. M. Bockman and J. K. Kochi, *J. Am. Chem. Soc.*, 1996, **118**, 3842.

Paper 8/09595G